Conductive and Transparent Multilayer Films for Low-Temperature-Sintered Mesoporous TiO_2 Electrodes of Dye-Sensitized Solar Cells

Seigo Ito,[†] Tetsuya Takeuchi,[‡] Terumasa Katayama,[‡] Masato Sugiyama,[‡] Mizuho Matsuda,[§] Takayuki Kitamura,[§] Yuji Wada,[§] and Shozo Yanagida*[,§]

Venture Business Laboratory and Material and Life Science Engineering Department, Graduate School of Engineering, Osaka University, Suita, Osaka 565-0871, Japan, and Toukai Rubber Industries, Ltd., 3-1, Higashi, Komaki, Aichi 485-8500, Japan

Received October 24, 2002. Revised Manuscript Received March 27, 2003

Conductive transparent thin films made of multilayer coatings consisting of three alternative layers (TiO_2/Ag/TiO_2, TAT) have been applied to dye-sensitized solar cells (DSCs). We have used sputtering deposition to prepare the transparent layers and measured the optical properties. Mesoporous TiO_2 electrodes for DSCs were coated on TAT by a spin-coating and low-temperature sintering method. They were compared to well-known transparent metal oxide glasses (ITO and F-doped SnO_2). These DSCs on the TAT coatings yielded a short-circuit photocurrent density of 9 mA/cm^2, a photocurrent of 700 mV, and an overall cell efficiency of 3.9% at one sun light intensity.

Introduction

Dye-sensitized solar cells (DSCs) using mesoporous TiO_2 electrodes are regarded as a promising alternative to silicone-type solar cells because of their low-cost fabrication.[1−9] Recently, plastic DSCs have attracted much more attention from the viewpoint of the fabrication of less weighty solar cells, and low-temperature sintering of nanostructured TiO_2 on plastic transparent substitutes made from Sn-doped In_2O_3 (also called ITO) has been reported.[8,9] However, plastic ITO layers on plastic substrates exhibit relatively high electrical resistance (sheet resistance, 60 Ω/□[9]), because favorable low resistance can be obtained upon high-temperature sputtering (>300 °C).

In an effort to produce conductive and transparent substrates, multilayer coatings consisting of dielectric material/metal/dielectric material have been developed, as exemplified by ZnS/Ag/ZnS,[10] ZnO/Ag/ZnO,[11] ITO/Ag/ITO,[11] and ITO/CuAg/ITO.[12] These multilayer transparent film layers have low reflectance, good transparency, and high conductivity when prepared using a low-temperature sputtering deposition. These multilayer transparent films have been studied with the aim of developing functional materials such as heat mirrors.[13−19]

In this work, multilayer transparent conductive coatings (dielectric material/metal/dielectric material) were fabricated for low-temperature-sintered electrodes of mesoporous TiO_2 in DSCs. TiO_2 was chosen as the dielectric material because of its high refractive index, its transparency in the visible region, and its easy sputtering. In addition, Ag was chosen as the conductive layer because of its low absorption in the visible region. Hence, TiO_2/Ag/TiO_2 transparent films (abbreviated as TAT) were fabricated, and their application to DSCs was examined.

In view of low-temperature sintering for the fabrication of mesoporous TiO_2 electrodes, it is favorable not to use organic surfactants and/or thickeners in making the initial TiO_2 colloidal solutions. Without such organic additives, however, it is difficult to make thick mesoporous TiO_2 electrodes (>5 μm).[8,9] In this work, to

* To whom correspondence should be addressed. E-mail: yanagida@mls.eng.osaka-u.ac.jp; Fax: 00-81-(0)6-6879-7875.
[†] Venture Business Laboratory, Osaka University.
[‡] Toukai Rubber Industries, Ltd.
[§] Material and Life Science Engineering Department, Graduate School of Engineering, Osaka University.

(1) O'Regan, B.; Grätzel, M. *Nature (London)* **1991**, *353*, 737.
(2) Nazzerruddin, M. K.; Kay, A.; Podicio, I.; Humphy-Baker, R.; Müller, E.; Liska, P.; Vlachopoulos, N.; Grätzel, M. *J. Am. Chem. Soc.* **1993**, *115*, 6382.
(3) Kalyansundaram, K.; Grätzel, M. *Coord. Chem. Rev.* **1998**, *77*, 347.
(4) Bach, U.; Lupo, D.; Comte, P.; Moser, J. E.; Weissörtel, F.; Salbeck, J.; Spreitzer, H.; Grätzel, M. *Nature (London)* **1998**, *395*, 583.
(5) Ito, S.; Ishikawa, K.; Wen, C.-J.; Yoshida, S.; Watanabe, T. *Bull. Chem. Soc. Jpn.* **2000**, *73*, 2609.
(6) Ito, S.; Kitamura, T.; Wada, Y.; Yanagida, S. *Solar Energy Mater. Solar Cells* **2003**, *76*, 3.
(7) Kambe, S.; Nakade, S.; Wada, Y.; Kitamura, T.; Yanagida, S. *J. Mater. Chem.* **2002**, 723.
(8) Pichot, F.; Pitts, J. R.; Gregg, B. A. *Langmuir* **2000**, *16*, 5626.
(9) Lindström, H.; Holmberg, A.; Magnusson, E.; Lindquist, S.-E.; Malmqvist, L.; Hagfeldt, A. *Nano Lett.* **2001**, *1*, 97.
(10) Leftheriotis, G.; Papaefthimou, S.; Yianoulis, P. *Solid State Ionics* **2000**, *136−137*, 655.
(11) Kusano, E.; Kawaguchi, J.; Enjouji, K. *J. Vac. Sci. Technol. A* **1986**, *4*, 2907.
(12) Bender, M.; Seelig, W.; Daube, C.; Frankenberger, H.; Ocker, B.; Stollemwerk, J. *Thin Solid Films* **1998**, *326*, 67.
(13) Chiba, K.; Nakatani, K. *Thin Solid Films* **1984**, *112*, 359.
(14) Dima, I.; Popescu, B.; Iova, F.; Popescu, G. *Thin Solid Films* **1991**, *200*, 11.
(15) Fan, J. C. C.; Bachner, F. J.; Foley, G. H.; Zavracky, P. M. *Appl. Phys. Lett.* **1974**, *25*, 693.
(16) Fan, J. C. C.; Bachner, F. J. *Appl. Opt.* **1976**, *15*, 1012.
(17) Eisenhammer, T.; Lazarov, M.; Leutbecher, M.; Schöffel, U.; Sizmann, R. *Appl. Opt.* **1993**, *32*, 6310.
(18) Fu, J. K.; Atanassov, G.; Dai, Y. S.; Tan, F. H.; Mo, Z. Q. *J. Non-Cryst. Solids* **1997**, *218*, 403.
(19) Lee, C.-C.; Chen, S.-H.; Jang, C.-C. *Appl. Opt.* **1996**, *35*, 5698.

10.1021/cm021051t CCC: $25.00 © 2003 American Chemical Society
Published on Web 06/18/2003

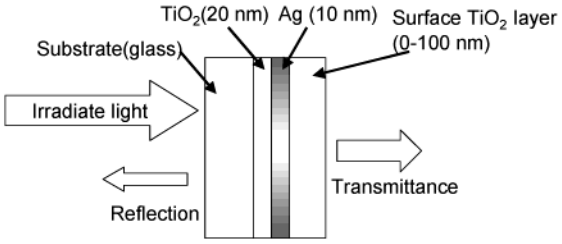

Figure 1. Structure of transparent film (TiO_2/Ag/TiO_2, TAT). Each layer was fabricated using a sputtering method.

increase the thickness of the mesoporous TiO_2 electrodes for DSCs (2.5−16 μm), a repeat spin-coating method was employed using a TiO_2 (P-25 and ST-41) paste without any organic additives. Because the aim was the fabrication of plastic DSCs using a TAT-covered PET, the sintering in the preparation of the mesoporpous TiO_2 electrodes was done under low-temperature conditions (150 °C). Although the TAT layer can be fabricated on plastic PET films, these conductive and transparent films were mainly fabricated on glass substrates so that TAT could be compared with other transparent conductive oxides [ITO and FTO (F-doped SnO_2)] used so far.[8,9] The TAT films, the low-temperature-sintered mesoporous TiO_2 electrodes on TAT films, and the DSCs using the mesoporous TiO_2/TAT electrodes were characterized by transmission/refraction spectroscopy in the visible region, transmission electron microscopy (TEM), scanning electron microscopy (SEM), and photovoltaic measurements.

Experimental Section

Materials. Nanocrystalline TiO_2 (P-25, Degussa, d = 21 nm), submicron TiO_2 particle (ST-41, Ishihara Sangyo, d = 200 nm), LiI (Wako Chemicals), and *cis*-bis(isothiocyanato)-bis(2,2′-bipyridyl-4,4′-dicarboxylato)ruthenium(II) bis(tetrabutylammonium) (Solalonix) were used as received. Iodine (Nacalai Tesque) was purified by sublimation. H_2O, *tert*-butylpyridine (Aldrich), and methoxyacetonitrile (Tokyo Chemical Industry) were purified by distillation. Dimethylpropylimidazolium iodide (DMPImI) was prepared from dimethylpropylimidazolium bromide (Shikoku Kasei) by ion exchange. Two types of transparent conducting oxides on glass (FTO: 10 Ω/□, Nippon Sheet Glass; ITO: 8 Ω/□, Kuramoto Co., Ltd.) were used as the substrate compared to TAT.

Fabrication of TiO_2/Ag/TiO_2 (TAT) Transparent Films. We used sputtering deposition techniques to prepare these TiO_2/Ag/TiO_2 (TAT) coatings using a DC sputtering system (SPW-025S, ULVAC). The TiO_2 layers were fabricated by a reactive sputtering method using a Ti target (99.9%, Kojundo Chemical Laboratory Co., Ltd.) under a mixed gas of O_2 (1.1 kgf m^{-2}, 560 sccm) and Ar (1.1 kgf m^{-2}, 110 sccm). The Ag layers were sputtered using an Ag target (99.99%, Sumitomo Metal Mining) under Ar gas (1.1 kgf m^{-2}, 250 sccm). All TAT coatings were deposited on 1-mm-thick glass. The thickness of each TAT film was controlled by the deposition time. Figure 1 shows the configuration of the TAT films. The thicknesses of the glass-attached TiO_2 layer and the Ag layer were fixed to 20 and 10 nm, respectively. The thickness of the surface TiO_2 layer was varied from 0 to 100 nm. The sheet resistance of each transparent film was 8 Ω/□ as determined using a 4-pin probe constant-current method (Loresta-GP MCP-T600, Mitsubishi Chemical Co., Ltd.). This resistance resulted from the thickness of the Ag layer. A transmission and reflectance spectrometer (UV-3100PC, Shimadzu) was used for the measurement of the optical properties of the thin transparent film. Taking into account the direction of the incident light for such a film used as a transparent film for DSCs, the incident light for each optical measurement was introduced from the glass substrate.

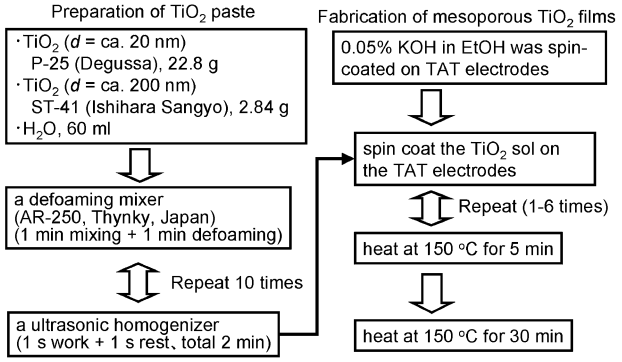

Figure 2. Fabrication scheme of mesoporous TiO_2 electrodes under low-temperature sintering on TAT films.

Coating of Mesoporous TiO_2 Electrodes. Figure 2 shows the procedure to fabricate mesoporous TiO_2 electrodes on the TAT film. P-25 (22.8 g), ST-41 (2.84 g), and H_2O (60 mL) were mixed using two systems: a defoaming mixer (AR-250, Thinky) and an ultrasonic homogenizer with a titanium horn (US-300T, Nihonseiki Kaisha Ltd.). The agitations using these two systems were alternatively repeated 10 times, and the coating paste was obtained.

A drop of a KOH solution (0.05% in ethanol) was set on the center of a conducting glass substrate (2.5 × 3.5 cm^2; TAT, FTO, and ITO) and flattened using a spin-coating method at 1000 rpm (ASS-301, ABLE Co., Ltd.). The KOH-treated substrates were then completely covered with the TiO_2 colloidal solution, spun at a speed of 1000 rpm, dried using an air drier, and heated at 150 °C for 5 min. After the first coating, the thickness of the resulting mesoporous TiO_2 electrodes was 2.5 μm. To increase the thickness of the mesoporous TiO_2 electrodes, the spin-coating and heat treatment were alternately repeated on the transparent film, and finally, the resulting TiO_2 mesoporous electrodes were sintered in air at 150 °C for 30 min. These TAT films with mesoporous TiO_2 electrodes, in view of conductivity, can withstand heating to 150 °C in air.

The morphology and thickness of the mesoporous TiO_2 electrodes were characterized using a scanning electron microscope (SEM; JEOL, JSM-6700F) and a surface profiler (Dektac 3), respectively.

Fabrication and Characterization of the DSCs. To protect the Ag layer from the iodine in the electrolyte, a thick TiO_2 surface layer (100 nm) on the TAT was used. The DSC configuration was as follows: ⟨glass/TiO_2 (20 nm, sputtering)/Ag (20 nm, sputtering)/TiO_2 (100 nm, sputtering)/mesoporous TiO_2 (2.5−16 μm, spin-coating)/Ru dye/liquid electrolyte/Pt/F-doped SnO_2/glass⟩. After the mesoporous TiO_2 electrodes on TAT had been heated at 150 °C for 30 min, the porous TiO_2 electrodes were cooled to 80 °C and immersed in an ethanol solution of a ruthenium complex [*cis*-bis(isothiocyanato)-bis(2,2′-bipyridyl-4,4′-dicarboxylato)ruthenium(II) bis(tetrabutylammonium)] at 80 °C for 3 h for dye adsorption. The dye-adsorbed TiO_2 electrodes were assembled into a sandwich-type cell. Pt-sputtered FTO glass served as the counter electrode. Two clips were used to press together the dyed electrode and the counter electrode. A drop of electrolyte solution (0.1 M LiI, 0.3 M DMPImI, 0.05 M I_2, and 0.5 M *tert*-butylpyridine in methoxyacetonitrile) was introduced into the clamped electrodes. The active area of the DSCs was ca. 0.4 cm^2 (ca. 0.4 × ca. 1.0 cm^2, with each length measured using a digital micrometer). Photocurrent−voltage measurements were performed using an AM 1.5 solar simulator (100 mW cm^{-2}, Yamashita Denso).

Results and Discussion

Optical Spectroscopy of Conductive and Transparent Layers: TAT, FTO, and ITO. Figure 3 shows the reflection spectra of TAT coatings (the thickness of

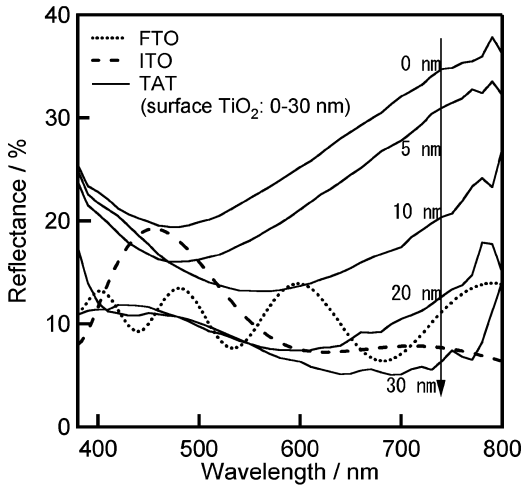

Figure 3. Reflectance spectra of TAT with surface TiO_2 layers (0, 5, 10, 20, and 30 nm), FTO, and ITO.

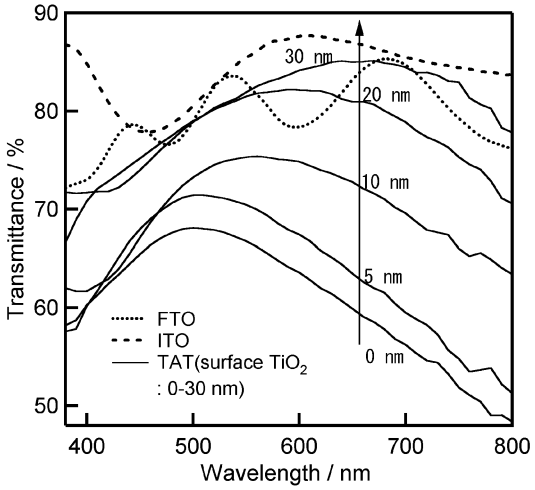

Figure 4. Transmittance spectra of TAT with surface TiO_2 layers (0, 5, 10, 20, and 30 nm), FTO and ITO.

the surface TiO_2 layer was varied from 0 to 30 nm), FTO, and ITO (see in Figure 1). The thickness of the surface TiO_2 layer affected the reflectance of the incident light from the glass substrate. The reflectance decreased gradually with increasing thickness of the surface TiO_2 layer on TAT, and the peak of the reflectance minimum moved to higher wavelengths. At a TiO_2 surface layer thickness of 30 nm, the reflectance of TAT was suppressed more than those of FTO and ITO.

Figure 4 shows the transmission spectra of the transparent films measured in Figure 3. The transmittance of TAT improved with decreasing reflectance related to the increase in the thickness of the surface TiO_2 layer (Figure 3). The transmittance of TAT with a TiO_2 surface layer thickness of 30 nm was comparable to those of FTO and ITO, which suggests together with the good conductivity (8 Ω/□), that the TAT should be useful for application to DSCs as a substitute for FTO and ITO.

Figure 5 shows the changes in transmittance and reflectance (on average at $\lambda = 400-700$ nm) of TAT with increasing thickness of the surface TiO_2 layer. The optimum values of the transmittance and reflectance occur for coatings with 25−35 nm of surface TiO_2. The transmittance and reflectance of TAT deteriorate at

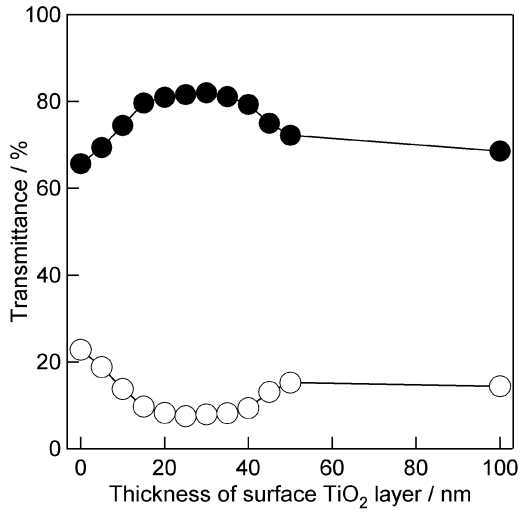

Figure 5. Relationship of the transmittance (●) and reflectance (○) of TAT to the thickness of the surface TiO_2 layer.

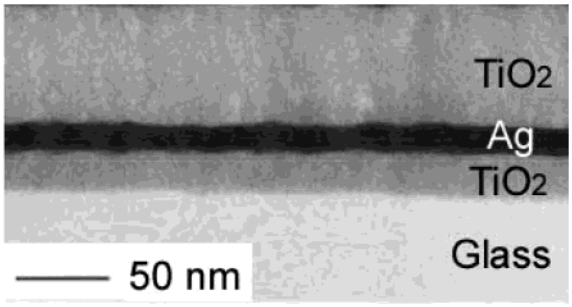

Figure 6. TEM image of the cross section of a TAT film.

TiO_2 surface layer thicknesses of more than 35 nm because of interference in the surface TiO_2 layer (>35 nm). However, TiO_2 surface layer thicknesses in TAT of over 50 nm affected the reflectance/transmittance only slightly, as seen in Figure 5. The TAT with the thicknesses 20 nm TiO_2/10 nm Ag/30 nm TiO_2 was found to show the optimum transmittance of 0.82 and reflectance of 0.063.

Morphologies of TAT and Mesoporous TiO_2 Layers. Figure 6 presents TEM images of a cross section of a TAT film on a glass substrate. Thes images confirm that each layer, TiO_2 and Ag, has a flat and smooth structure, which suggests high conductivity at the Ag layer of TAT. Transparent conductive multilayers (dielectric/Ag/dielectric) fabricated using sputter-coating[11,12] have a lower resistance than those prepared by vacuum thermal evaporation methods.[10] The difference comes from the morphology of the Ag layer. The Ag layer prepared using vacuum thermal evaporation forms an island structure.[14] The low contact between each Ag island grain results in a high resistivity. On the other hand, the Ag layer prepared by sputter-coating is smooth and has a low resistivity. Because the TAT in this report was prepared by the sputter-coating method and has a low resistivity (8 Ω/□ for a 10-nm thickness of the Ag layer), the Ag layer in the TAT was flat and smooth enough to make it attractive for use as a transparent film.

Figure 7a and b presents SEM images of the surface and cross section, respectively, of a mesoporous TiO_2 electrode (prepared with four cycles of coating) on TAT. The surfaces of the mesoporous TiO_2 electrodes were

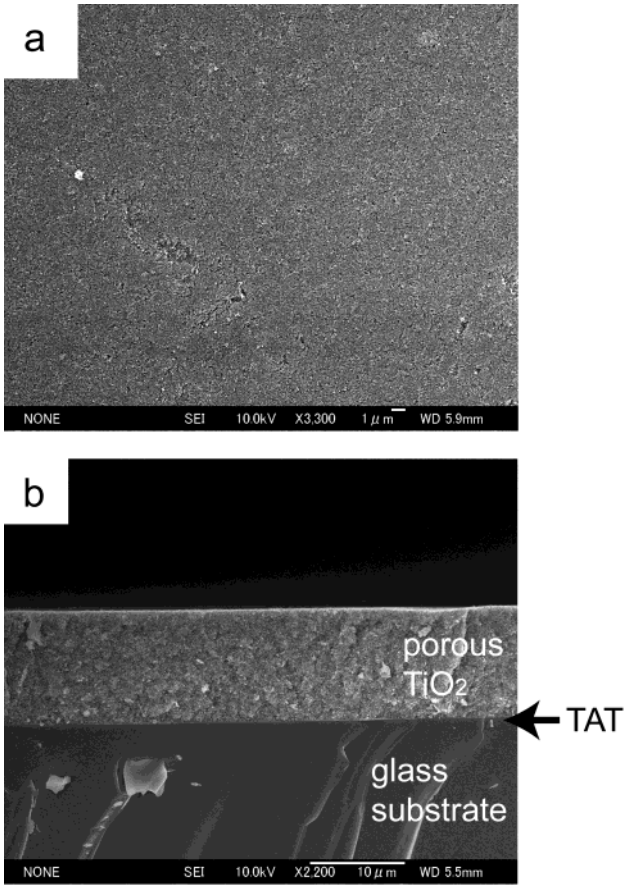

Figure 7. SEM images of the (a) surface morphology and (b) cross section of a mesoporous TiO_2 electrode [four spin-coating and drying (150 °C) cycles] on TAT film.

found to be smooth enough for use as electrodes in DSCs (Figure 7a). Without treatment with KOH/ethanol solution on the surface of the TAT (see Figure 2), the resulting TiO_2 electrodes had large cracks on the surface, probably as a result of a lack in cohesion at the interface between TAT and TiO_2 nanocrystallites. The thickness of the porous electrode after four cycles of coating (thickness = ca. 10 μm) gave a homogeneous cross section (Figure 7b), and no traces of a boundary phase were observed in the cross-section image between adjacent pairs of layers caused by the repeated spin-coating (Figure 7b). On the other hand, for the mesoporous TiO_2 prepared by a repeated doctor-blade coating and drying (80 °C) method using organic additives in a TiO_2 colloidal paste, we observed gaps and boundary layers between the repeated doctor-blade-coated layers and also macropore structures and cracks on the surface after sintering.[6,7] The morphology of the present spin-coated mesoporous TiO_2 layers (see Figure 7) is quite comparable to that of TiO_2 layers obtained by a repeated doctor-blade coating and combustion (500 °C) method using a TiO_2 paste containing organic additives.[6] Hence, it was concluded that each nanocrystallite should be positioned evenly with the others despite the low-temperature sintering and that the absence of organic additives in the TiO_2 colloidal paste gave homogeneous and smoothly sintered electrodes after the lower-temperature sintering.

The present repeated doctor-blade coating and drying (150 °C) method enabled the fabrication of thick electrodes up to 16 μm. When compared to the thickness of the previously reported mesoporous TiO_2 electrodes prepared by low-temperature sintering (1[8] and 5 μm[9]), this method is appropriate for the fabrication of thicker mesoporous TiO_2 electrodes under low-temperature sintering.

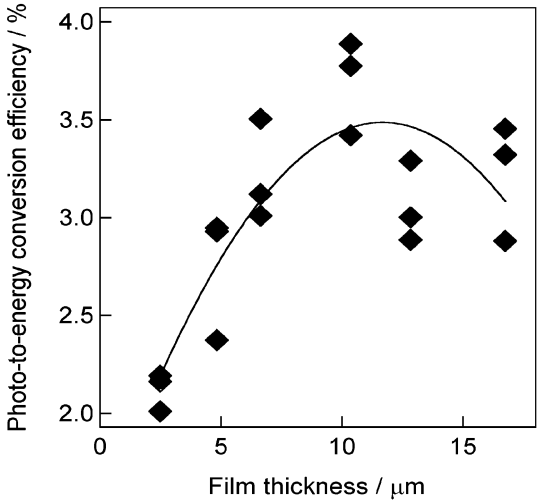

Figure 8. Relationship between the thickness of the mesoporous TiO_2 electrodes and the light-to-energy conversion efficiencies (η) of DSCs prepared on TAT films.

Characteristics of DSCs Fabricated Using TAT, FTO, or ITO Substrates. We have compared DSC performances of mesoporous TiO_2 electrodes prepared using TAT, FTO, and ITO as conductive and transparent substrates in DSCs. Regardless of the optimum thickness of the surface TiO_2 layer (30 nm) in the TAT film (see Figure 5), the TAT films with thick surface TiO_2 layers (100 nm) were used in the DSCs to protect the Ag layer in the TAT from corrosion by the iodine in the electrolyte. Hence, the structure of window-side DSC electrodes with TAT was ⟨TiO_2 (20 nm)/Ag (10 nm)/TiO_2 (100 nm)/nanocrystalline TiO_2 (2.5−16 μm)/Ru dye⟩. Despite the thick TiO_2 layer (100 nm) on the Ag layer, the Ag layer of the TAT underwent corrosion, being dissolved into the electrolyte, and the conductivity of the TAT decreased. Hence, photovoltaic measurements of DSCs using TAT were performed within 3 min of the injection of the iodine electrolyte.

Figure 8 shows the relation between the thickness of the mesoporous TiO_2 layers and the light-to-energy conversion efficiencies (η) of the DSCs using TAT. At 2.5 μm (one coating cycle), the η value was 2.01−2.19%. η was found to increase with increasing thickness of the surface TiO_2 layer, and at 10 μm (four coating cycles), there was a maximum η of 3.42−3.89%.

Figure 9 shows the light $I-V$ characteristics of the DSCs prepared using TAT, ITO, and FTO. The results displaye are the best cell performances obtained in the photovoltaic measurements of each of the three cells. The $I-V$ characteristics for the TAT are significantly improved compared over those for the ITO and FTO cases (Table 1). The improvement in the conversion efficiency depends not on the differences in the conductivities of the transparent layers (TAT, 8 Ω/□; ITO, 8 Ω/□; and FTO, 10 Ω/□) but on the antireflection (AR) ability of the TAT layers (Figure 3) and the transmittance of the incident light. It is known that the introduction of AR films on solar cells can increase the

Table 1. *I*−*V* Characteristics of DSCs Fabricated Using FTO, ITO, and TAT and the Mesoporous TiO_2 Electrodes Obtained by Four Cycles of Spin-Coating and Drying (150 °C), Measured under AM 1.5 (100 mW cm^{-2})[a]

	transparent film		
	FTO	ITO	TAT
J_{SC} (mA cm^{-2})	6.89 (6.70−7.09)	7.15 (6.73−7.76)	9.79 (8.39−11.92)
V_{OC} (mV)	686 (681−693)	678 (674−681)	746 (0.741−0.751)
FF	0.684 (0.683−0.685)	0.636 (0.630−0.645)	0.516 (0.422−0.575)
η (%)	3.22 (3.13−3.31)	3.09 (2.85−3.34)	3.69 (3.42−3.89)

[a] Data are based on the averages of three dye-sensitized cell samples; ranges of data are shown in parentheses.

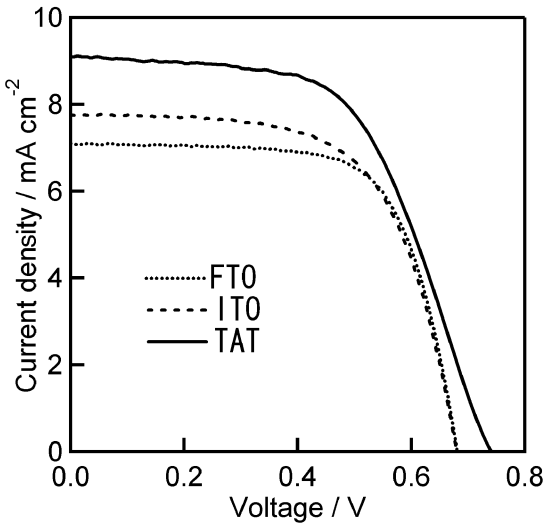

Figure 9. Light *I*−*V* characteristics of DSCs prepared using TAT, ITO, and FTO (four spin-coating and drying cycles). Each curve comes from the best cell of that type in terms of the conversion efficiency determined by photovoltaic measurements.

photovoltaic performance of the cells.[20] Proper arrangement of the thickness of each layer in the TiO_2/Ag/TiO_2/nanocrytalline TiO_2/Ru dye stack to suppress internal reflections achieves a high photocurrent and conversion efficiency of the DSC; the mesoporous TiO_2 electrode on the TAT film can make a continuous structure of TiO_2 and cancel the refracting interface, resulting in an increase in the absorption of the incident light by the Ru dyes that generate the high photocurrent. To reinforce this argument, it would be useful to include the reflectance/transmittance spectra of the transparent films with the mesoporous TiO_2 electrodes, such as reported by Tachibana et al., who used an integrating sphere inside a UV−vis absorption spectrometer.[21] However, because the optical thicknesses of the mesoporous TiO_2 electrodes prepared in this work were very large because of the large TiO_2 particles (ST-41) used in making these electrodes, the distinct differences in the reflectance/transmittance spectra with these mesoporous TiO_2 electrodes were impossible to detect, so no discussion of this issue is included here.

DSCs prepared using thick mesoporous TiO_2 electrodes (10 μm) under low-temperature sintering on FTO and ITO achieved conversion efficiencies of 3.22 and 3.09%, respectively, under 1 sun (Table 1). The conversion efficiencies of DSCs prepared using FTO or ITO were larger than the reported data for low-temperature-sintered DSCs prepared using FTO (thickness of mesoporous TiO_2, 1 μm; efficiency, 1.22%)[8] or ITO (thickness of mesoporous TiO_2, 5 μm; efficiency, 2.3%).[9] The difference in the efficiencies was ascribed to the thickness of the mesoporous TiO_2 electrodes that were employed in the present work. Generally, the thick mesoporous TiO_2 electrodes give higher conversion efficiencies than the thin TiO_2 electrodes. The optimum thickness of the mesoporous TiO_2 electrode was determined to be 10 μm (Figure 7) in the present work.

Conclusions

The sputtering deposition technique has been applied to produce TiO_2/Ag/TiO_2 layers with favorable qualities: the sheet resistance was 8 Ω/□, and the average transmittance and reflectance (400−700 nm) were 82 and 6.3%, respectively. TiO_2 nanocrystallites were successfully deposited by repeated spin-coatings on conductive TAT layers for DSCs and sintered at 150 °C. The resulting mesoporous TiO_2 electrodes suppressed reflection losses of incident light energy, thus improving the performance of DSCs prepared using the low-temperature sintering method (average η = 3.69%). However, the Ag metal in TAT reacts with I_3^- in the electrolyte upon long-term usage. Therefore, when DSCs using nonhalogen electrolytes such as cobalt complexes[22,23] or solid-state hole-transport materials[4,24,25] are established, TAT can be used as a low-reflectance and transparent substrate for making improved DSCs or plastic DSCs.

CM021051T

(20) Cid, M.; Stem, N.; Brunetti, C.; Beloto, A. F.; Ramos, C. A. S. *Surf. Coat. Technol.* **1998**, *106*, 117.
(21) Tachibana, Y.; Hara, K.; Sayama, K.; Arakawa, H. *Chem. Mater.* **2002**, *14*, 2527.
(22) Nusbaumer, H.; Moser, J.-E.; Zakeeruddin, S. M.; Nazeeruddin, M. K.; Grätzel, M. *J. Phys. Chem. B* **2001**, *105*, 10461.
(23) Sapp, S. A.; Elliott, C. M.; Contado, C.; Caramori, S.; Bignozzi, C. A. *J. Am. Chem. Soc.* **2002**, *124*, 11215.
(24) Krüger, J.; Plass, R.; Cevey, L.; Piccirelli, M.; Grätzel, M.; Bach, U. *Appl. Phys. Lett.* **2001**, *79*, 2085.
(25) Krüger, J.; Plass, R.; Grätzel, M.; Matthieu, H.-J. *Appl. Phys. Lett.* **2002**, *81*, 367.